Mediation of Chemoattractant-induced Changes in $[Ca^{2+}]_i$ and Cell Shape, Polarity, and Locomotion by $InsP_3$, DAG, and Protein Kinase C in Newt Eosinophils

Susan H. Gilbert, Kristine Perry, and Fredric S. Fay

Department of Physiology and Program in Molecular Medicine, University of Massachusetts Medical Center, Worcester, Massachusetts 01605

Abstract. During chemotaxis large eosinophils from newts exhibit a gradient of $[Ca^{2+}]_i$ from rear to front. The direction of the gradient changes on relocation of the chemoattractant source, suggesting that the Ca^{2+} signal may trigger the cytoskeletal reorganization required for cell reorientation during chemotaxis. The initial stimulatory effect of chemoattractant on $[Ca^{2+}]_i$ and the opposite orientations of the intracellular Ca^{2+} gradient and the external stimulus gradient suggest that more than one chemoattractant-sensitive messenger pathway may be responsible for the generation of spatially graded Ca^{2+} signals. To identify these messengers, Ca^{2+} changes were measured in single live cells stimulated with spatially uniform chemoattractant. On stimulation spatially averaged $[Ca^{2+}]_i$ increased rapidly from $\leqslant$100 nM to $\geqslant$400 nM and was accompanied by formation of lamellipods. Subsequently cells flattened, polarized and crawled, and $[Ca^{2+}]_i$ fluctuated around a mean value of $\sim$200 nM. The initial Ca^{2+} spike was insensitive acutely to removal of extracellular Ca^{2+} but was abolished by treatments expected to deplete internal Ca^{2+} stores and by blocking receptors for inositol-trisphosphate, indicating that it is produced by discharge of internal stores, at least some of which are sensitive to $InsP_3$. Activators of protein kinase C (PKC) (diacyl glycerol and phorbol ester) induced flattening and lamellipod activity and suppressed the Ca^{2+} spike, while cells injected with PKC inhibitors (an inhibitory peptide and low concentrations of heparin-like compounds) produced an enhanced Ca^{2+} spike on stimulation. Although cell flattening and lamellipod activity were induced by chemoattractant when the normal Ca^{2+} response was blocked, cells failed to polarize and crawl, indicating that Ca^{2+} homeostasis is required for these processes. We conclude that $InsP_3$ acting on Ca^{2+} stores and DAG acting via PKC regulate chemoattractant-induced changes in $[Ca^{2+}]_i$, which in turn control polarization and locomotion. We propose that differences in the spatial distributions of $InsP_3$ and DAG resulting from their respective hydrophilic and lipophilic properties may change Ca^{2+} distribution in response to stimulus reorientation, enabling the cell to follow the stimulus.

DIRECTIONAL persistence during locomotion in a stimulus gradient and rapid reorientation when the direction of the stimulus gradient changes are virtually certain to involve a complex web of highly interactive intracellular processes that stabilize directionality in a way that can be immediately and effectively overridden. Although components of the signal transduction pathways that control cell orientation have been identified in many types of cells, little is known about the mechanisms involved in translating the spatio-temporal patterns of the stimulus into appropriate changes in intracellular organization. The ubiquity of pathways in which Ca^{2+} serves as a second messenger and the Ca^{2+}-sensitivity of a large number of cytoskeletal proteins suggests that Ca^{2+} could play an important role. Thus considerable effort has been devoted to characterizing changes in the spatial distribution of $[Ca^{2+}]_i$ in response to agonists and understanding their physiological significance (e.g., Albritton and Meyer, 1993; Girard and Clapham, 1993; Thorn et al., 1993).

Large free-living amebae often exhibit a gradient of $[Ca^{2+}]_i$, with the highest concentration in the rear of the cell (except during phagocytosis, when $[Ca^{2+}]_i$ rises in the region of the presumptive phagosome; Taylor et al., 1980). A similar Ca^2 gradient in newt eosinophils reverses direction when the stimulus gradient is reversed during chemotaxis (Brundage et al., 1991). Many proteins that affect the organization of the actin cytoskeleton are sensitive to $[Ca^{2+}]$ (e.g., Yin and Stossel, 1979), and $[Ca^{2+}]$ has opposite effects on

Address all correspondence to Dr. Susan H. Gilbert, Department of Physiology and Program in Molecular Medicine, University of Massachusetts Medical Center, 373 Plantation Street, Worcester, MA 01605. Telephone: (508) 856-6908; FAX: (508) 856-1840.

the ATPase activities of myosin II and some isoforms of myosin I (Collins and Matsudaira, 1991; see Pollard and Korn, 1973). The two types of myosin are distributed differently in locomotory cells, myosin I being confined mostly to the front of the cell and myosin II to the rear (Fukui et al., 1989). An in vitro contraction model consisting of a gel of myosin II and actin mixed with filamin and gelsolin contracts away from the high concentration end of a $[Ca^{2+}]_i$ gradient (Janson et al., 1991). The spatial distribution of the Ca^{2+}-calmodulin complex, which likely reflects the distribution of its activated target proteins, including those that activate myosin II, is similar to that of $[Ca^{2+}]_i$ in migrating fibroblasts, as demonstrated with a fluorescent analog of calmodulin (Hahn et al., 1992). Ca^{2+} also seems to play a role, via integrins, in regulating the attachment of human neutrophils to the substratum (Marks et al., 1991). Collectively these observations suggest that a gradient of $[Ca^{2+}]_i$ could stabilize the organization of cytoskeletal components responsible for cell polarity.

They also raise the question of how the spatial pattern of $[Ca^{2+}]_i$ itself arises. In secretory epithelia (see Thorn et al., 1993), the $[Ca^{2+}]_i$ gradient results from spatial variations in the density of $InsP_3$-sensitive internal stores. In newt eosinophils during chemotaxis, however, the direction of the $[Ca^{2+}]_i$ gradient changes rapidly in response to relocating the stimulus source (within tens of seconds; Brundage et al., 1991) and well before the cell reorientation which enables it to follow the stimulus. Thus $[Ca^{2+}]_i$ must be controlled at least partly by messenger pathways that allow spatial characteristics of the stimulus to be translated acutely into a new spatial distribution of Ca^{2+}. Brundage et al. (1993) showed that fluctuations in $[Ca^{2+}]_i$ appear to correlate with changes in cell shape, speed, and orientation. The next step toward understanding the origin and the physiological significance of the $[Ca^{2+}]_i$ gradient is to identify chemoattractant-sensitive messengers that affect Ca^{2+} homeostasis and to determine how they might produce particular spatial patterns of $[Ca^{2+}]_i$.

These experiments were designed to determine whether chemoattractant-induced changes in $[Ca^{2+}]_i$ result from influx across the plasma membrane or discharge of internal stores or both, to identify which if any of the most common second messengers affect $[Ca^{2+}]_i$ and to investigate the relation between changes in $[Ca^{2+}]_i$ and cell shape, polarity, and locomotion when $[Ca^{2+}]_i$ was perturbed by experimental intervention. Newt eosinophils injected with fura-2 were activated with chemoattractant applied uniformly in the medium (to evoke chemokinesis) and stimulus-sensitive second-messenger pathways identified by quantifying changes in $[Ca^{2+}]_i$ in response to treatments expected to alter these pathways. Cell morphology and locomotion were monitored simultaneously. The results show that chemoattractant-induced increases in $[Ca^{2+}]_i$ can originate exclusively from internal stores, at least some of which appear to be sensitive to inositol-1,3,4-biphosphate ($InsP_3$)[1]. The data also suggest that diacyl glycerol (DAG) and protein kinase C (PKC) activity suppress $[Ca^{2+}]_i$. Ca^{2+} homeostasis appears to be required for polarization and locomotion but not for cell activation and flattening. Both Ca^{2+} and PKC activity seem to affect cell shape. A scheme is proposed for messenger-mediated changes in the spatial distributions of $[Ca^{2+}]_i$ and PKC activity in response to changes in the external chemoattractant gradient during chemotaxis, by means of which these two agents could serve as initiators of cell reorientation, perhaps overriding spatial patterns arising from variations in the density of Ca^{2+} stores.

Materials and Methods

Cell Preparation and Experimental Protocols

Newt eosinophils were prepared by a modification of the technique of Koonce et al. (1984). Newts were bled by clipping the tip of the tail and 0.2–0.3 ml of blood collected in 1 ml heparinized amphibian culture medium (ACM, pH 7.2, and containing, mM: 64 NaCl, 4.3 KCl, 1.4 $CaCl_2$, 1.3 $MgSO_4$, 0.7 NaH_2PO_4, 19.2 Hepes and 4.4 glucose). 0.1 ml of the mixture was spread on a 25-mm circular coverslip. Cells settled and attached in ~30 min. The coverslip was washed in ACM to remove erythrocytes and clamped into a frame to form a cell chamber, which was filled with 0.4–0.6 ml ACM and mounted on the stage of an inverted microscope. During the first 5–10 min on the microscope, most cells were polarized and active and became quiescent over the next 10–15 min, first withdrawing lamellipods, and then becoming round and loosening attachments to the substrate. Cells were injected as they were undergoing this process, using a Picospritzer II (General Valve Corp., E. Hanover, NJ). The injectate contained 0.5–1.0 mM fura-2 (potassium salt) dissolved in 20 mM Pipes or 10 mM glutamic acid/potassium glutamate (pH 7.2). When necessary, the cells were allowed to recover until $[Ca^{2+}]_i$ was ≤100 nM (10–20 min). Cell volume was ~4 pl, injection volume ≤8% cell volume and $[\text{fura-2}]_i$ <40 μM unless otherwise indicated. Methods used to determine these values are described below.

Phase-contrast images were acquired at 0.5 s^{-1} and fura-2 fluorescence image pairs at 0.1 s^{-1}. The basic experimental protocol was to record images as ACM was replaced with 10% newt serum in ACM (the only substance known to be chemotactic for these cells; see Brundage et al., 1993), with various agents added either to the injectate or to the bathing medium. At least one cell from each blood sample was injected with fura-2 alone and treated only with 10% newt serum and the data used to assess other "control" treatments, such as injection with nominally inactive peptides and other agents and exposure to the solvents of drugs introduced into the medium.

Chemicals

Chemicals were purchased from Sigma Chem. Co. (St. Louis, MO). PKC inhibitor peptide (PKC[19-36]), protein kinase A inhibitor peptide (PKA[6-22]amide) and PKC non-inhibitory analog peptide ([glu^{27}]PKC[19-36]) were from GIBCO BRL (Gaithersburg, MD).

Imaging and Data Analysis

Phase-contrast and fluorescence images at excitation wavelengths of 340 and 380 nm were acquired using the Digital Imaging Microscope described by Brundage et al. (1991) and a Nikon 40× UVF objective (NA 1.4). The modified Zeiss IM35 inverted microscope was equipped with two cameras. A video camera (Dage MTI CCD72, Michigan City, IN, from which the infra-red filter was removed) passed to a video disk recorder (Panasonic TQ-2028F) phase-contrast images acquired using transmitted illumination through a 680-nm high-pass filter. A low noise, slow-readout, thermoelectrically cooled CCD camera (model CH220, TI 4849 detector, Photometrics, Tucson, AZ) acquired fura-2 fluorescence image pairs that were transferred directly to the disk of a PDP-11/73 microcomputer (Digital Equipment Corporation, Maynard, MA). A mask in the optical path to the cooled CCD camera allowed only half the chip to be exposed. The image acquired at the first excitation wavelength (filter 340/DF10 nm; Omega Optical, Brattleboro, VT) was shifted electronically to the masked half of the chip as the second excitation filter (380/DF10 nm) was being positioned. The duration of each exposure was 0.5 s and the interval between the two images of a pair 0.1 s. The size of each pixel in the fluorescence image was 0.526 μm and the size of the field read from the CCD controller onto computer disk 100

1. *Abbreviations used in this paper*: ACM, amphibian culture medium; DAG, diacyl glycerol; DOG, dioctanoyl glycerol; $InsP_3$, inositol-1,3,4-biphosphate; PKC, protein kinase C; SPS, sulfated polysaccharides.

× 150 μm (one-quarter of the chip) for the image at each excitation wavelength. The PDP-11/73 controlled the cooled CCD camera shutter, image transfer from the CCD chip to disk, the excitation filter wheel and shutter (MVI, Avon, MA) and phase-contrast image acquisition by the video disk recorder. All analysis was performed on Silicon Graphics Personal Iris workstations (Mountain View, CA), connected to the PDP via Ethernet, using software developed in the laboratory. Phase-contrast images stored on video disk were digitized by the image acquisition interface of a Silicon Graphics GTX workstation. Images were stored on erasable optical laser disks (Introl Corp., Minneapolis, MN). Composite $[Ca^{2+}]_i$ and phase-contrast images were generated with Silicon Graphics UNIX utilities software and 35-mm photographic film exposed by a Matrix Color Graphic Recorder (Agfa, Matrix Division, Orangeburg, NY) interfaced to a Personal Iris.

Computation of $[Ca^{2+}]_i$. Image pairs of fura-2 fluorescence at λ_{ex340} and λ_{ex380} were stored by the camera controller on hard disk as an alternating time-lapse series. Background fluorescence was determined by averaging intensities of a 4400-pixel region of the field never entered by the cell during recording, and that value was subtracted from each pixel of each image in the sequence. The concentration of Ca^{2+} at each pixel was then calculated from the relation developed by Tsien and coworkers (Grynkiewicz et al., 1985; see Moore et al., 1990). The spatially averaged $[Ca^{2+}]_i$ values shown in the graphs were calculated by averaging $[Ca^{2+}]_i$ values of all pixels within the perimeter of the cell, which was marked by an automated tracing program based on a threshold/flood-fill algorithm, operating on the bleach-corrected, Ca^{2+}-insensitive fura-2 images calculated as described below.

Determination of Intracellular Concentrations of Injectate Constituents

A procedure was developed for quantifying the intracellular concentrations of fura-2 and other injected compounds, based on the fact that many cells were spherical until exposed to chemoattractant. Thus cell volume could be calculated by measuring cell diameter in phase-contrast or fluorescence images. The optical system was calibrated by injecting a cell-sized microdroplet of fura-2 into silicone oil in the cell chamber (Moore et al., 1990). Phase-contrast images of the spherical droplet were recorded by time-lapse video as the pipette was lowered to the bottom glass surface of the chamber. The volume of the microdroplet was calculated from sphere diameter measured from the video images. When the droplet contacted the glass surface, it adhered and flattened to form a disk whose total intensity was recorded with the cooled CCD camera, at the same exposure and camera gain used in cell experiments. The area of the field from which fluorescence intensity was recorded was 200 × 150 μm and so included the entire region surrounding the fluorescent disk. Background fluorescence at both wavelengths was recorded from an empty field and subtracted before further data processing. The calibration factor (CF) for fura-2 is given by

$$\text{CF (mol/count)} = \frac{\text{[fura-2] (mol/liter} \times \text{sphere volume (1)}}{\text{microdroplet intensity (counts).}} \quad (1)$$

Diameters of spherical cells were measured from fluorescence images and the intracellular concentration of fura-2 calculated from

$$[\text{fura-2}]_{\text{cell}}\ \text{(mol/liter)} = \frac{\text{cell intensity (counts)} \times \text{CF (mol/count)}}{\text{cell volume (1).}} \quad (2)$$

Intensities in both equations are the Ca^{2+}-insensitive values calculated from the 340 and 380 image pairs (to avoid recording a third image at the isosbestic wavelength of fura-2), given by

$$I = I_{340} + (I_{380} \times B), \quad (3)$$

where B is the ratio of the dynamic range of the 340 to the 380 fluorescence intensity determined by calibrating fura-2 in solutions of $<10^{-7}$ and $>10^{-3}$ M $[Ca^{2+}]$ on the microscope (Becker and Fay, 1987). Intracellular concentrations of other components of the injectate were calculated from their ratio to fura-2 concentration in the injectate, assuming this ratio to be unaffected by experimental protocols.

Introduction of Drugs into the Medium

Extracellular agents were introduced by replacing the bathing medium. In the case of acute presentation of 5 mM EGTA to reduce extracellular $[Ca^{2+}]$, it was essential to determine the time required for $[Ca^{2+}]$ immediately adjacent to the cell to become less than resting intracellular $[Ca^{2+}]$. Normal medium containing fura-2 was added to the chamber with activated uninjected cells and the kinetics of the decrease in $[Ca^{2+}]$ next to a cell recorded as this medium was replaced with new medium containing the same concentration of fura-2 and 5 mM EGTA. The field diaphragm in the epifluorescence excitation path was focused on the coverslip and constricted to illuminate a region ~30 μm in diameter, producing the quasi-confocal optical conditions required to record fluorescence from a layer of solution ≤20-μm deep at the surface of the coverslip (see Hiraoka et al., 1990). The thickness of this layer was verified independently as follows. The cell was positioned so that part of its anterior granule-containing region occupied ~30% of the illuminated field. Upon changing the medium, external $[Ca^{2+}]_i$ fell from >1 mM to <1 μM within 10 s and to <50 nM within 20 s. The actual depth of the in-focus solution layer that contributed significantly to the fura-2 fluorescence images was assessed by monitoring the decrease in fluorescence intensity in focal planes above the coverslip as the objective was moved upward and the image of the field diaphragm became blurred. Simultaneous phase-contrast images of the cell recorded by the video camera showed that when the top (medium-facing) surface of the cell was optimally focused (~10 μm above the coverslip), fluorescence intensity had decreased by >50%. Thus, fura-2 fluorescence ≥10 μm above the coverslip did not contribute significantly to the fluorescence used to calculate $[Ca^{2+}]$ just outside the cell, which was much less than cytoplasmic $[Ca^{2+}]$ when Ca^{2+} spikes occurred in cells injected with fura-2 and recorded as they were exposed to medium containing 5 mM EGTA.

Results

Chemoattractant Causes $[Ca^{2+}]_i$ to Increase and Cells to Flatten, Polarize, and Crawl

When resting eosinophils were exposed to chemoattractant, the first response was a sudden transient increase in $[Ca^{2+}]_i$ by several hundred nM, followed by flattening, polarization (i.e., expansion of a single advancing lamellipod at one end, constriction of the cell cortex and location of the nucleus at the other) and locomotion. These events are illustrated in the first two figures, showing a series of phase-contrast and $[Ca^{2+}]_i$ images of a typical cell (Fig. 1) and a graph of spatially averaged $[Ca^{2+}]_i$ from the same cell (Fig. 2). Lamellipods are apparent in the phase-contrast image acquired at the peak of the initial Ca^{2+} transient (Fig. 1, 20 s). As the cell began to elongate away from the nuclear region, a $[Ca^{2+}]_i$ gradient formed (70–90 s). The rate of decline in $[Ca^{2+}]_i$ was spatially graded, being highest where lamellipods were forming (compare $[Ca^{2+}]_i$ images at 70, 80, and 90 s). As was typical for these cells, the $[Ca^{2+}]_i$ gradient from front to rear was largest when average $[Ca^{2+}]_i$ was highest, <100 at 420 and ~250 nM at 450 s.

Both the kinetics and the spatial characteristics of the responses were consistent from cell to cell, except as noted. In 46 cells, resting $[Ca^{2+}]_i$ (averaged for 1–2 min before stimulation) was 85 ± 5 nM (mean ± standard error). Peak $[Ca^{2+}]_i$ in response to chemoattractant was 417 ± 16 nM (defined as the maximal value within 2 min of stimulation) and the time to peak 34 ± 3 s. The range of activation peaks was broad (214–708 nM), and in many cells, $[Ca^{2+}]_i$ rose from the resting level to the peak within one 10-s interval, suggesting that sampling frequency was too low for the true peak to be recorded. Other cells, like that shown in Fig. 1, produced several spikes within 2 min of stimulation, and occasionally the initial spike was not the largest. The postactivation level of $[Ca^{2+}]_i$ was 201 ± 12 nM (29 cells), averaged for 1 min between the Ca^{2+} spikes that occurred in most cells during chemokinesis. For example, $[Ca^{2+}]_i$ val-

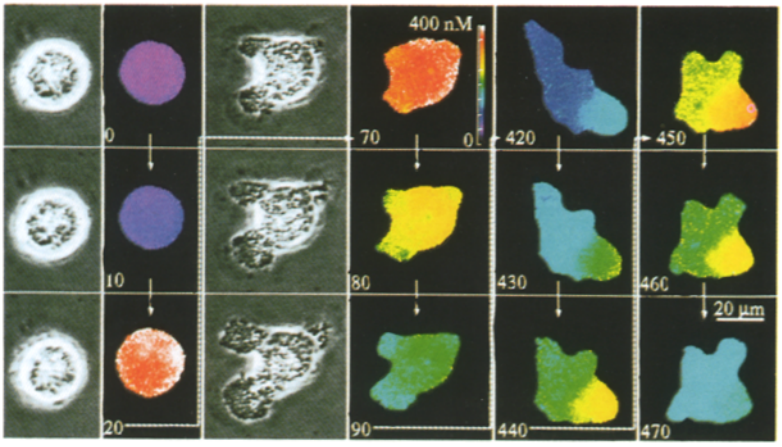

Figure 1. Phase-contrast and Ca^{2+} images of a cell activated by chemoattractant. Phase-contrast images at only the first six time points are shown. Times in seconds after introducing chemoattractant by changing the medium are shown in the lower left corner of each Ca^{2+} image. Simultaneous phase-contrast and fluorescence images were acquired and $[Ca^{2+}]_i$ calculated as described in Materials and Methods. Arrows indicate image sequence in time. In this and all subsequent figures showing $[Ca^{2+}]_i$ images, the units of the $[Ca^{2+}]_i$ scale (image at 70 s) are in nM and the linear scale bar ($[Ca^{2+}]_i$ image at 470 s) is 20 μm.

ues for the cell in Figs. 1 and 2 were averaged between 6 and 7 min after activation to determine the postactivation level.

Included in these mean values are data from seven cells injected with the inactive analog of the peptide inhibitor of PKC, two cells injected with the peptide inhibitor of cAMP-dependent protein kinase, one cell exposed to 0.1% DMSO (the solvent for several agents added to the medium), four cells exposed to 1,3-dioctanoyl glycerol (DOG) (a diacyl glycerol not found in live cells), and 2 cells injected with de-N-sulfated heparin, a control compound for the sulfated-polysaccharide $InsP_3$ receptor blockers. None of these cells was different from the other 30 cells, which were injected with fura-2 alone and exposed only to ACM and 10% newt serum.

Some cells did not flatten and move across the substrate in response to chemoattractant but instead elongated vertically into the medium with only the nuclear end attached. Although these cells were actively changing shape, horizontal velocity in the plane of the substrate was near zero, and, except for the initial spike, $[Ca^{2+}]_i$ was well below active levels measured in crawling cells. Some of these cells eventually flattened and crawled, and this change was accompanied by an increase in $[Ca^{2+}]_i$, suggesting that Ca^{2+} changes and locomotion are tightly coupled. The only $[Ca^{2+}]_i$ values from these "swimming" cells included in the mean values given above are resting and peak values, which were within the range of the other control cells. None of the agents used to perturb $[Ca^{2+}]_i$ in the experiments to be described affected the frequency with which this type of response occurred. It was observed less often when the coverslips were washed in hot 5 N HCl.

$[Ca^{2+}]_i$ measured within 1 min of injection with fura-2 was often higher than values recorded 10–20 min later, probably because of Ca^{2+} influx produced by injection. Cells with postinjection values of 0.5–1 μM usually flattened, polarized, and crawled for a few minutes. As $[Ca^{2+}]_i$ declined, some of these cells resumed their original spherical shape, while others were tightly stuck to the coverslip and remained flattened but inactive, as indicated by the absence of lamelli-

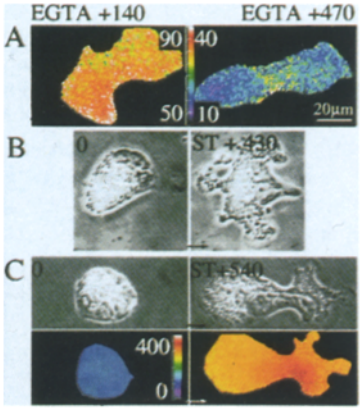

Figure 7. Images showing effects of Ca^{2+} depletion from internal stores and injection of exogenous Ca^{2+} buffer on responses to stimulation. The cell whose $[Ca^{2+}]_i$ image is shown in *A* is the same as that in Figs. 3 *C* and 4 *C*. The color bar in *A* has two different scales, from 50 to 90 nM for the image on the left, 140 s after EGTA application, and 10–40 nM for the image on the right, 470 s after EGTA. The cell in *B* was exposed to 5 mM EGTA for 20 min, which reduced $[Ca^{2+}]_i$ to <50 nM (Fig. 8. *A*) and blocked the stimulus-induced Ca^{2+} spike. The cell in *C* was injected with fura-2 to a final intracellular concentration of 55 μM, calculated as described in Materials and Methods. Pseudocolor images of $[Ca^{2+}]_i$ in *C* are for the cell shown in Fig. 8 *B*, and the color bar concentration scale is in nM. Note that the $[Ca^{2+}]_i$ scales are different in for *A* and *C*.

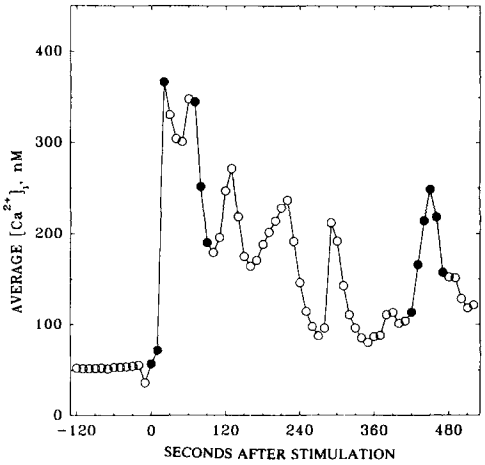

Figure 2. Time course of the Ca^{2+} response to chemoattractant stimulation. $[Ca^{2+}]_i$ values of all pixels within the cell shown in Fig. 1 were averaged at each time point to construct the graph, in which filled symbols correspond to the images shown in Fig. 1.

pods, shape changes, and locomotion. While the initial Ca^{2+} spike produced by activation of spherical cells appeared to be spatially uniform, in flattened cells it was spatially graded, with the highest $[Ca^{2+}]_i$ in the perinuclear region.

$[Ca^{2+}]_i$ Spikes Are Independent of Ca^{2+} Influx from the External Medium

The increase in $[Ca^{2+}]_i$ elicited by chemoattractant could come from influx across the plasma membrane, from discharge of internal stores, or both. Relative contributions of these two sources were assessed by measuring $[Ca^{2+}]_i$ in the presence of extracellular EGTA during random migration in spatially uniform chemoattractant (chemokinesis) and in response to stimulation. In 4 of 9 cells treated with 5 mM EGTA during chemokinesis, Ca^{2+} spikes and cell polarity and locomotion persisted for at least 10 min (the duration of the treatment after the recording period). The time course of changes in average $[Ca^{2+}]_i$ in one of these cells is shown in Fig. 3 *A* and phase-contrast micrographs in Fig. 4 *A*. In the other five cells, $[Ca^{2+}]_i$ declined and locomotion eventually ceased. The decline in $[Ca^{2+}]_i$ preceded changes in locomotion by several minutes, as shown by the graphs in Fig. 3, *B* and *C* and the phase-contrast micrographs in Fig. 4, *B* and *C*. In both cells $[Ca^{2+}]_i$ had dropped to <100 nM by the end of the recording period, but the latency between exposure to EGTA and the fall in $[Ca^{2+}]_i$ was longer and the rate of decline in $[Ca^{2+}]_i$ lower in 3 *B* than in 3 *C*. The disparity in the two Ca^{2+} responses correlated with differences in the extent of morphological changes apparent in the cells during the last 60 seconds of recording. The cell in Fig. 4 *B* seemed to have been in the process of reversing direction between 480 and 530 s after EGTA treatment, as indicated by the change in proximity of the granule-containing cytoplasm and phase-dark lamellipods to the left side of the images. The cell shown in Fig. 4 *C* had already lost its leading lamellipod 440 s after exposure to EGTA and between 440 and 500 s pulled its nuclear region forward to lie beneath the phase-bright granule-containing region. Both cells had become completely nonmotile 5–10 min after the end of recording. Thus in cells that are fully polarized and active, $[Ca^{2+}]_i$ was not acutely affected by removing Ca^{2+} from the medium. However, once $[Ca^{2+}]_i$ did fall, the cells ultimately stopped moving and lost polarity, although there was a significant delay between the reduction in $[Ca^{2+}]_i$ and the loss of polarity and motility.

Another feature of the Ca^{2+} responses of activated cells to EGTA treatment was the persistence of the Ca^{2+} gradient until average $[Ca^{2+}]_i$ had declined to 50–100 nM, as illustrated by Ca^{2+} images in Fig. 7 *A*. (The time course of spatially averaged $[Ca^{2+}]_i$ in the same cell is shown in Fig. 3 *C* and phase-contrast images in Fig. 4 *C*). About 2 min after EGTA treatment (*image on left*, pseudocolor scale 50–90 nM), cytoplasmic $[Ca^{2+}]$ was ~10 nM higher in the perinuclear region than in the front of the cell. After ~8 min, however, spatially averaged $[Ca^{2+}]_i$ had dropped to <60 nM (Fig. 3 *C*), and $[Ca^{2+}]_i$ was <40 nM in most regions of the cell (Ca^{2+} image on the right, ranged of $[Ca^{2+}]_i$ on the pseudocolor scale 10–40 nM, below the level reliably quantifiable with fura-2). One interpretation of the persistence of the gradient of $[Ca^{2+}]_i$ to the lower limit of

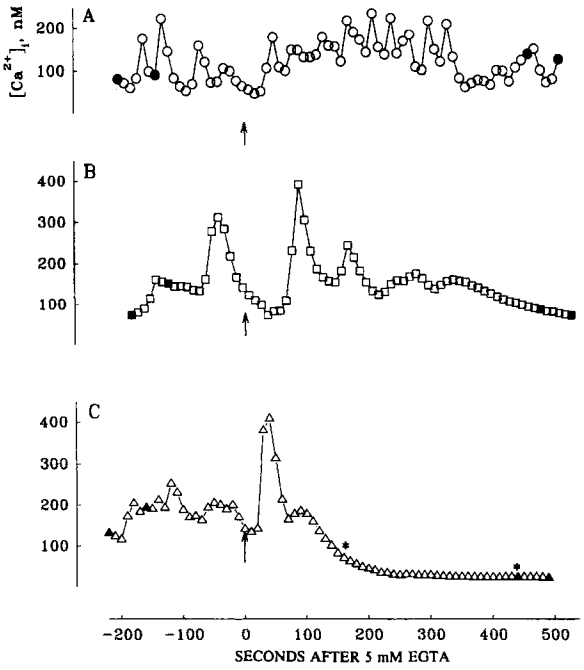

Figure 3. Time course of changes in $[Ca^{2+}]_i$ in three cells before and after removal of extracellular $[Ca^{2+}]_i$. Spatially averaged $[Ca^{2+}]_i$ values are from three cells recorded during chemokinesis as medium containing 5 mM EGTA was introduced. Filled symbols indicate time points of phase-contrast images shown in Fig. 4, asterisks in *C*, the time points of Ca^{2+} images shown in Fig. 7 *A*.

detection with fura-2 is that Ca^{2+} storage sites are most dense in the perinuclear region.

Another group of cells was exposed to 5 mM EGTA before activation with chemoattractant. In general, treatment with EGTA for a few minutes produced no effect on the initial Ca^{2+} response to chemoattractant stimulation, although longer treatments depleted internal stores, as described in the following section. The graph in Fig. 5 shows the Ca^{2+} response of a cell incubated in EGTA for 10 min, and then activated by chemoattractant. The cell produced a robust initial Ca^{2+} spike followed by several smaller ones before $[Ca^{2+}]_i$ ultimately declined to ≤50 nM. Thus the Ca^{2+} spike produced by stimulation does not require Ca^{2+} influx across the plasma membrane. The phase-contrast micrographs of this cell in Fig. 6 show that although its initial morphological response to stimulation was normal, it failed to polarize, inset, in that its nucleus assumed a position in the center of the cell and lamellipods formed simultaneously at several locations and extended in many directions. Also the cell never crawled. These responses were typical of three other cells exposed for 2–10 min to EGTA before stimulation.

Ca^{2+} Homeostasis Is Required for Polarization and Locomotion but Not for Flattening and Lamellipod Extension

To learn which chemoattractant-induced morphological changes were sensitive to $[Ca^{2+}]_i$, some cells were treated with EGTA for ≥15 min and others injected with fura-2 to high intracellular concentrations (55–400 μM) to buffer changes in free $[Ca^{2+}]_i$. The effects of EGTA are shown by the phase-contrast images in Fig. 7 *B*. The cell was slightly

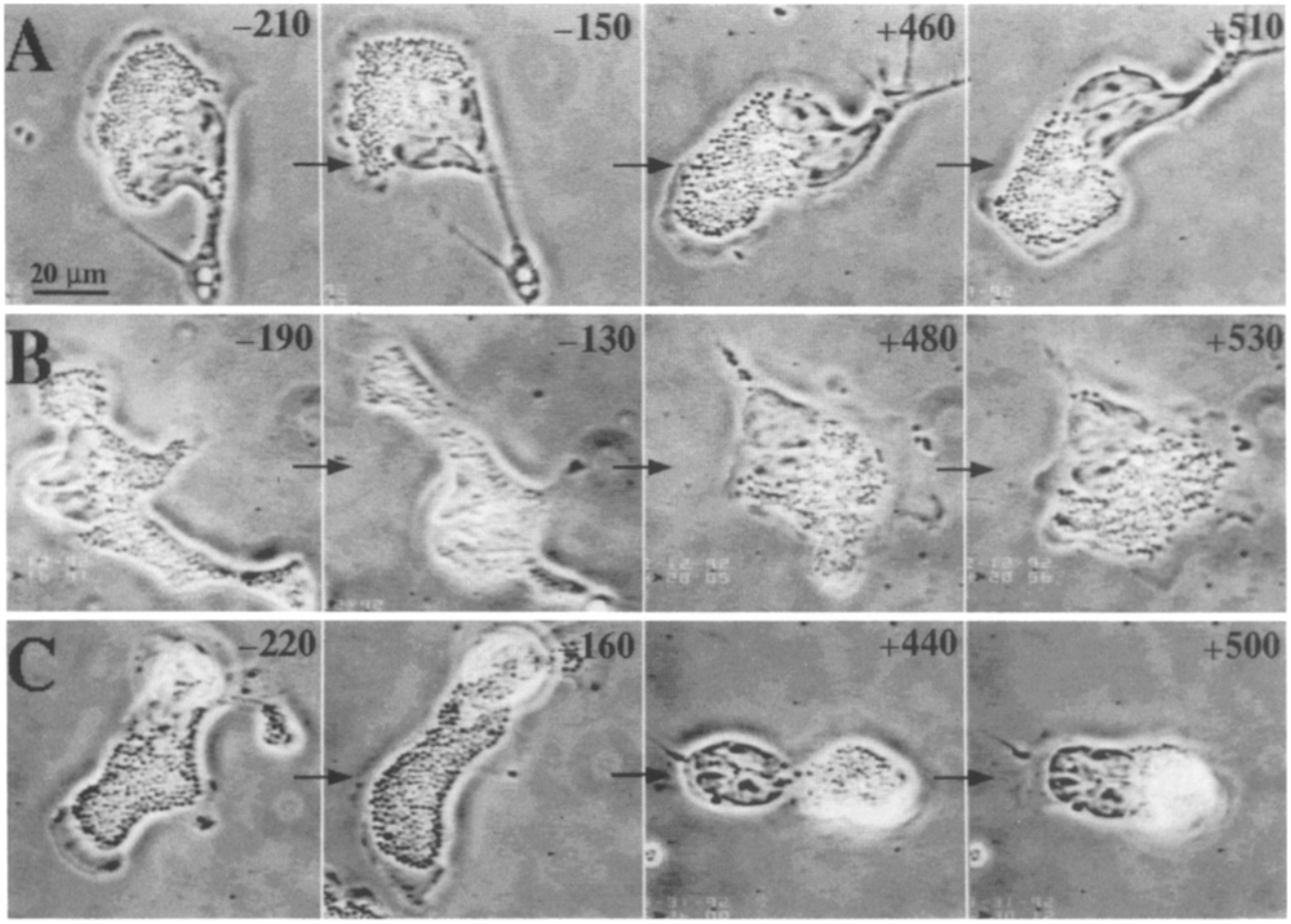

Figure 4. Phase-contrast images of three cells showing effects of removing extracellular Ca^{2+} on cell shape and locomotion during chemokinesis. Times are in seconds relative to removal of external Ca^{2+} by introducing medium containing both 10% newt serum and 5 mM EGTA. The scale bar in the image of cell *A* at −210 s is 20 μm. The arrows show the image sequence.

flat and polarized at the time of stimulation (0 s), as shown by the elongated shape and the location of the nucleus at one end, but inactive, as indicated by the absence of lamellipods and shape changes in the phase-contrast video record (not shown). On stimulation, the cell flattened further and extended lamellipods in several directions away from the cytoplasmic extension containing the nucleus. There was no detectable change in $[Ca^{2+}]_i$ during the 10-min recording period after stimulation with chemoattractant (Fig. 8 *A*).

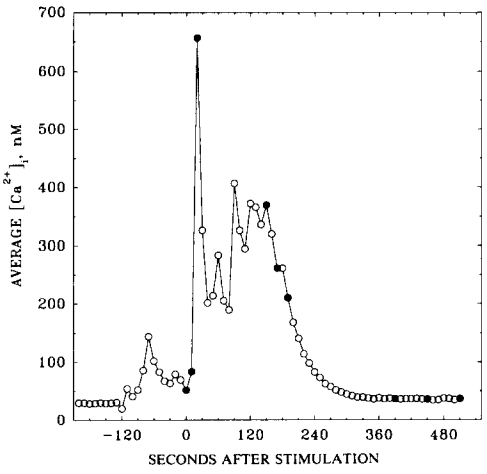

Figure 5. Ca^{2+} response to stimulation in Ca^{2+}-free medium. Time course of changes in average $[Ca^{2+}]_i$ during activation after exposure to 5 mM EGTA for 10 min. Filled symbols indicate time points corresponding to phase-contrast micrographs in Fig. 6.

The cell in Fig. 7 *C* was injected with 1 mM fura-2 to a final intracellular concentration of 55 μM. As shown by the graph in Fig. 8 *B*, $[Ca^{2+}]_i$ rose slowly to reach a peak of 400 nM 2.5 min after stimulation. The distribution of $[Ca^{2+}]_i$ at 540 s is typical of the pattern observed throughout the stimulus post-recording period, with $[Ca^{2+}]_i$ highest in the perinuclear region. This cell also failed to polarize, in that the nucleus became centrally located, and although the cell elongated, lamellipods formed at both ends of the long axis.

Sulfated Polysaccharide Blockers of $InsP_3$ Receptors Obliterate Both the Ca^{2+} Spike and Morphological Responses to Chemoattractant

The fact that discharge of internal stores is sufficient to produce increases in $[Ca^{2+}]_i$ in response to chemoattractant suggests that the effect could be mediated by $InsP_3$. Cells were therefore injected with one of several sulfated polysaccharides (SPS), which block binding of $InsP_3$ to its receptor (EC_{50} 6.9 μg/ml for pentosan polysulfate on $InsP_3$ receptors from liver microsomes; Tones et al., 1989; see

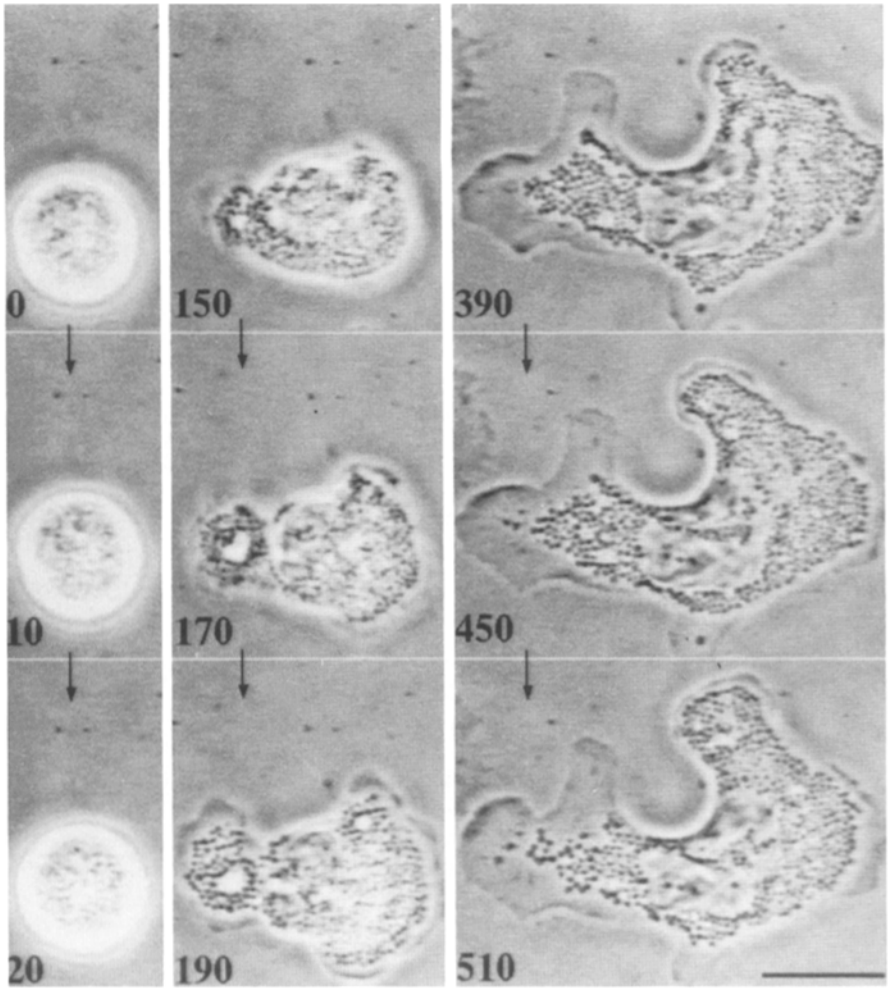

Figure 6. Phase-contrast images of a cell stimulated in Ca^{2+}-free medium. Times are in seconds relative to stimulus application, and the arrows show image sequence in time. $[Ca^{2+}]_i$ during 12 min of recording before and after stimulation of the same cell is shown in Fig. 5.

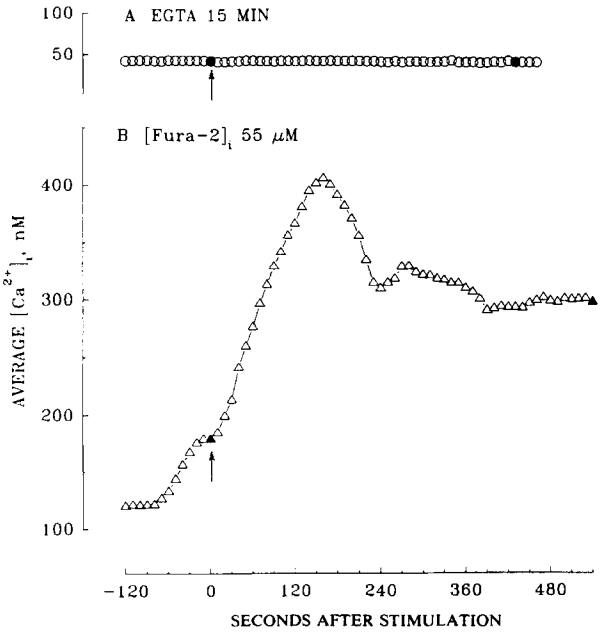

Figure 8. Time course of Ca^{2+} responses to stimulation after depletion of internal stores by exposure to EGTA or injection with excess fura-2. Data are from cells shown in Fig. 7. Arrows indicate when chemoattractant was added, and filled symbols corresponding to spatially averaged $[Ca^{2+}]_i$ values of the images shown in Fig. 7.

also Ghosh et al., 1988; Hill et al., 1987). Phase-contrast and $[Ca^{2+}]_i$ images of two cells injected with fura-2 and either heparan sulfate or an inactive heparin analog, de-N-sulfated heparin, are shown in Fig. 9. In contrast to the inactive compound (Figs. 9 *B* and 10 *B*), heparan sulfate completely abolished the Ca^{2+} response to chemoattractant (Fig. 10 *A*). Identical results were obtained with heparin sulfate and pentosan polysulfate.

The phase-contrast images in Fig. 9 *A* show that the heparan-injected cell also exhibited no morphological response to chemoattractant. This result was surprising in view of the persistence of chemoattractant-induced shape changes under conditions in which Ca^{2+} responses to chemoattractant were altered by injection of high concentrations of fura-2 or prolonged exposure to EGTA (Fig. 7). Thus the sulfated polysaccharides blocked not only the Ca^{2+} spike but also Ca^{2+}-independent flattening and lamellipod extension. Several investigators have reported that sulfated polysaccharides inhibit PKC (K_i for pentosan polysulfate in vitro 0.32 μg/ml; Herbert and Maffrand, 1991). The ubiquity of the coproduction of diacyl glycerol and $InsP_3$ by receptor-mediated activation of phospholipase C in chemoattractant-activated cells (see Lew, 1989) and the stimulatory effects of PKC on actin polymerization (Zimmerman and Keller, 1988) suggest that the DAG/PKC pathway could be responsible for the morphological changes seen on stimulation in the absence of a Ca^{2+} spike (Fig. 7 *B*). Given the

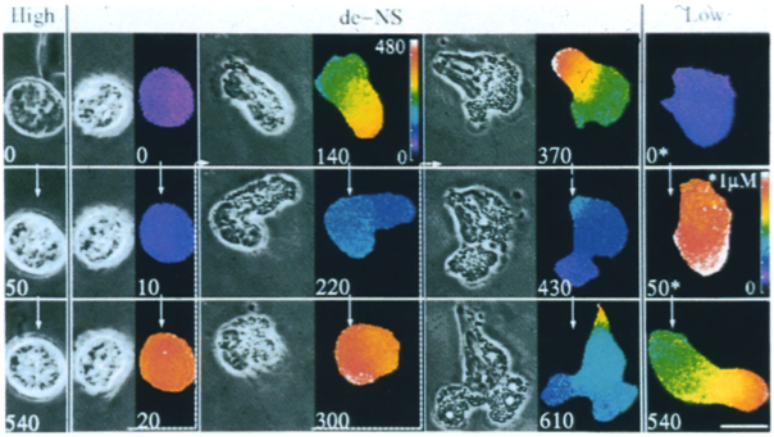

Figure 9. Effects of sulfated polysaccharides on chemoattractant-induced changes in cell shape and $[Ca^{2+}]_i$. Phase-contrast images of a cell injected with heparan sulfate (intracellular concentration ~108 μg/ml) and stimulated with chemoattractant are shown in the left column. Micrographs in the three double panels in the center show phase-contrast and $[Ca^{2+}]_i$ images from a cell injected with de-N-sulfated heparin (*de-NS*) (intracellular concentration ~104 μg/ml). The time course of changes in average $[Ca^{2+}]_i$ in each cell is shown in Fig. 10. The scale bar in the $[Ca^{2+}]_i$ image at 540 s is 20 μm. The right column shows Ca^{2+} images of a cell injected with pentosan polysulfate (intracellular concentration ~1.3 μg/ml), and then activated with 10% newt serum. The images at time points flagged with an asterisk (0, 50 s) are displayed with the $[Ca^{2+}]_i$ scale whose maximum value is 1 μM (50 s). The last image, 540 s after stimulation, is displayed with a $[Ca^{2+}]_i$ scale whose maximum is 480 nM (140 s).

difference in affinities of these compounds for PKC and the $InsP_3$ receptor, they would inhibit the $InsP_3/Ca^{2+}$ and DAG/PKC pathways at high intracellular concentrations (Figs. 9 *A* and 10 *A*) but at low concentrations would block only the DAG/PKC pathway. To test this idea, cells from the same blood samples were injected with SPS at concentrations in the injectate of either 0.05 or 2 mg/ml. On stimulation, cells injected with the low dose flattened, polarized, and crawled normally and were morphologically indistinguishable from control cells. The three Ca^{2+} images of such a cell in Fig. 9 *C* show that both resting $[Ca^{2+}]_i$ and the initial spike produced by the chemoattractant stimulus were significantly higher than in control cells. The time-averaged $[Ca^{2+}]_i$ during chemokinesis was slightly higher, although the difference was not significant, as shown by the bar graph in Fig. 11, which summarizes results from several experiments. Thus injecting cells with SPS to intracellular concentrations below their affinity for the $InsP_3$ receptor inhibited a pathway, possibly leading to activation of PKC, that normally limits the amplitude of the Ca^{2+} spike. These results suggest that both $InsP_3$ and PKC participate in chemoattractant stimulation and that PKC activity may suppress $[Ca^{2+}]_i$.

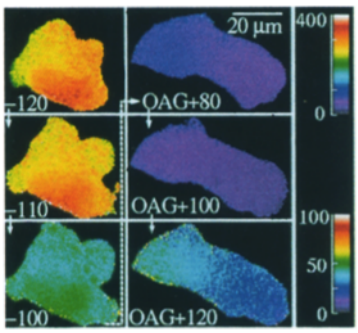

Figure 17. Effect of a diacyl glycerol on $[Ca^{2+}]_i$ in an active cell during chemokinesis. A fully active cell in 10% newt serum in ACM was injected with fura-2 and acquisition of phase-contrast and fura-2 fluorescence images acquired as described in Materials and Methods. During recording, octanoyl-acetyl glycerol (*OAG*) was added by swapping the medium for the same medium which included the DAG at a concentration of 100 μM.

Injection of a Peptide Inhibitor of PKC Potentiates the Ca^{2+} Response to Chemoattractant

To demonstrate directly the effects of PKC inhibition, cells were injected with a peptide that comprises the autoinhibitory domain of the enzyme. Chemoattractant-induced changes in $[Ca^{2+}]_i$ are shown in Fig. 12. The cell in *A* was injected with the inhibitor peptide, the cell in *B* with an inactive control peptide. Both cells produced a Ca^{2+} spike within 30 s of chemoattractant application. However, the magnitude of the spike was more than three times larger in the cell injected with the inhibitor peptide, similar to the observations with low intracellular concentrations of SPS. No obvious differences were observed between the morphologi-

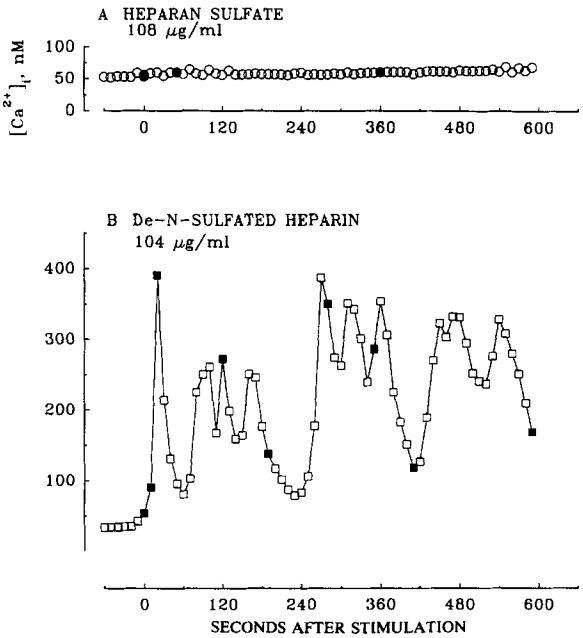

Figure 10. Effect of injection of heparan sulfate or de-N-sulfated heparin on the time course of the Ca^{2+} response to stimulation. The intracellular concentrations shown in the graph legends of heparan and de-N-sulfated heparin were calculated as described in Materials and Methods.

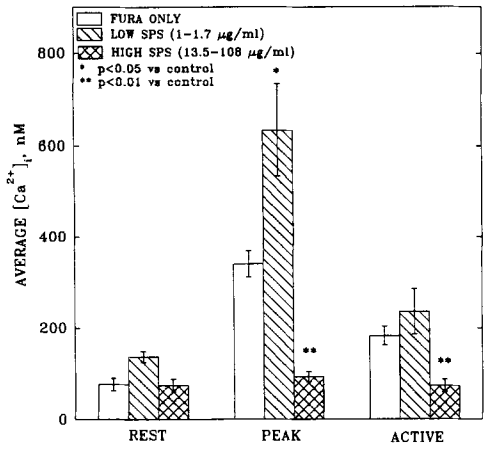

Figure 11. Concentration-dependent effects of sulfated polysaccharides on chemoattractant-induced changes in cell shape and $[Ca^{2+}]_i$. Injectates contained: fura-2 only (0.5 mM, seven cells) or fura-2 + de-N-sulfated heparin (2 mg/ml, two cells); fura-2 + pentosan polysulfate (50 μg/ml, four cells, *low SPS*); or fura-2 + heparin sulfate (one cell), pentosan polysulfate (three cells), or heparan sulfate (two cells), all at 2 mg/ml. Intracellular concentrations of SPS were calculated from $[\text{fura-2}]_i$ as described in Materials and Methods, and their ranges are shown for each group in the inset. Bars are standard errors of the mean.

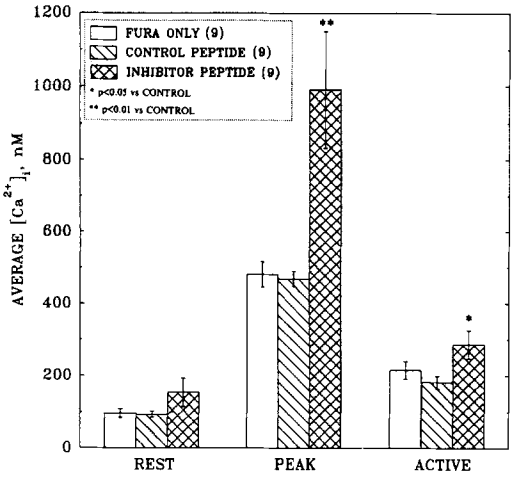

Figure 13. Effects of PKC inhibitory peptide on resting, peak, and active $[Ca^{2+}]_i$. Nine cells were injected with fura-2 alone, 9 with the peptide inhibitor of PKC, and 9 with the inactive peptide. Peptide concentration in the injectate was 5 mM. The range of $[\text{fura-2}]_i$ was 3–42 μM, of peptides, 27–424 μM. 12 of the 27 cells were spherical before activation (3 fura-2, 4 inactive peptide, 5 inhibitor peptide). Intracellular concentrations of fura-2 and peptide were estimated in the 15 nonspherical cells using the average volume calculated from the spherical ones.

cal or locomotory responses of cells injected with the inhibitor peptide and those of control cells. Velocities and turning frequencies were similar, as were the breadth, spatial distribution, and rate of formation of lamellipods.

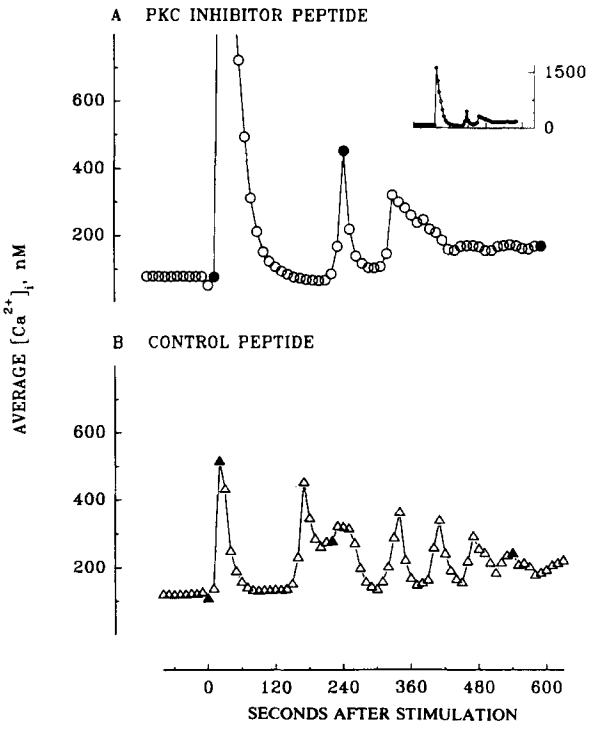

Figure 12. Effects of a peptide inhibitor of PKC on the Ca^{2+} response to chemoattractant. Fluorescence images were recorded 10–20 min after injection of cells with either a peptide inhibitor of PKC (*A*) or an analog peptide having a single amino acid substitution that blocks its inhibitory effect (*B*). The inset in *A* shows that $[Ca^{2+}]_i$ during the initial spike exceeded 1.5 μM.

Effects of injecting the PKC inhibitor peptide into several cells are summarized in Fig. 13. The high standard error in peak $[Ca^{2+}]_i$ in cells injected with the peptide is probably due to the low frequency of image acquisition in these experiments (0.1 s^{-1}). In many of these experiments, $[Ca^{2+}]_i$ reached its peak value within 10 s of stimulation, suggesting that the true maximal value was not recorded.

The mean values from cells injected with control peptide include measurements from two cells injected with a peptide inhibitor of cyclic AMP-dependent protein kinase. Although the intracellular concentration of this peptide was 100× that required for complete inhibition of its target enzyme, neither the Ca^{2+} response nor the behavior of the cells was distinguishable of those cells injected with fura-2 alone or with the inactive analog of the PKC inhibitor. This result is consistent with an earlier observation (Brundage et al., 1993) that agents that increase intracellular cAMP (other than caffeine) have no detectable effect on cell behavior and support the conclusion that neither cAMP nor cAMP-dependent protein kinase plays an important role in signal transduction in these cells. Furthermore, the results eliminate the possibility that the PKC inhibitor peptide had a nonspecific effect on cAMP-dependent kinase.

Activators of PKC Reduce $[Ca^{2+}]_i$ and Cause Flattening and Lamellipod Extension

If inhibition of PKC augments the chemoattractant-induced Ca^{2+} response, agents that stimulate PKC activity should reduce the amplitude of the Ca^{2+} spike produced by chemoattractant and perhaps elicit changes in cell shape in its absence. To test this possibility, PMA and a diacyl glycerol (1,2-dioctanoyl glycerol, 1,2-DOG) were applied to cells before activation by chemoattractant, as shown in Figs. 14 and 15. Phase-contrast (Fig. 14) and $[Ca^{2+}]_i$ images of a resting cell in ACM were recorded for 30 s, and then the cell was

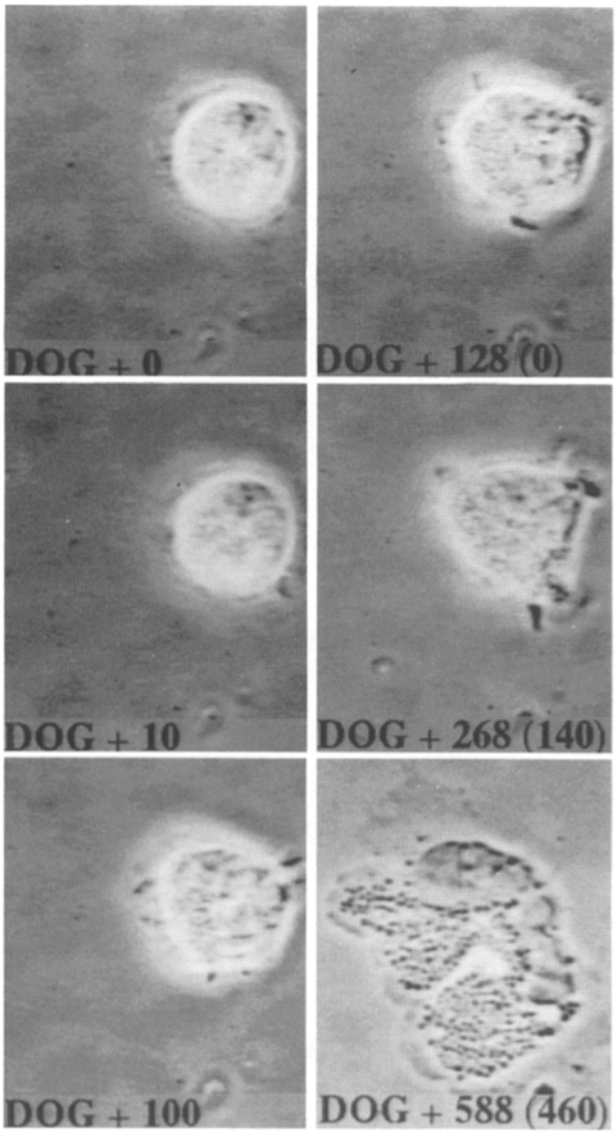

Figure 14. Effects of diacyl glycerol on morphological responses to chemoattractant. Phase-contrast images of a cell exposed for 128 s to 1,2-dioctanoyl glycerol, and then to 1,2-DOG + 10% newt serum. Times are in seconds relative to 1,2-DOG treatment or chemoattractant stimulation (in parentheses).

treated with 100 μM 1,2-DOG. Within 2 min lamellipod activity had increased, although, as shown by the graph in Fig. 15 *C*, $[Ca^{2+}]_i$ remained low. The cell was next stimulated with 10% newt serum (containing 1,2-DOG). Almost 4 min later $[Ca^{2+}]_i$ increased slightly, to ~250 nM. The cell never polarized and moved but instead situated its nucleus in the center and extended competing lamellipods from each end (Fig. 14).

Fig. 15 shows changes in average $[Ca^{2+}]_i$ in three other cells, one (*A*) preincubated in 1,3-DOG, a diacyl glycerol not known to occur in live cells, another (*B*) preincubated in 1,2-DOG, and the fourth (*D*) exposed acutely to 50 nM PMA. All treatments except 1,3-DOG significantly suppressed and delayed the Ca^{2+} response and stimulated lamellipod activity and some flattening but blocked polarization and locomotion.

A total of four 1,2-DOG-treated cells and four control cells were used in the experimental protocol illustrated in Figs. 14 and 15 *C*. As shown in the inset of Fig. 16, 1,2-DOG had no effect on resting $[Ca^{2+}]_i$ ($p > 0.5$ for paired observations). However, it did produce flattening and lamellipod activity in three of the four cells, while none of the control cells responded to replacing the medium. The cell shown in Fig. 14 exhibited the least flattening, but the most lamellipod activity, of the four cells treated acutely with 1,2-DOG. Shape changes induced by chemoattractant in cells pretreated with PKC activators were quite similar to those of Ca^{2+}-depleted cells.

Seven other 1,2-DOG-treated cells and nine controls were used in the protocol illustrated in Fig. 15 *B*, in which cells were preincubated in medium with or without 1,2-DOG before recording began. As there were no differences in the Ca^{2+} responses to chemoattractant in the 2-min and 10-min exposures to 1,2-DOG, results from experiments with the two protocols were pooled and are summarized in the large bar graph in Fig. 16. The suppression of the initial Ca^{2+} spike by 1,2-DOG is highly significant and leads to the same conclusion as the effects of PKC inhibitors, that a chemoattractant-induced increase in DAG and PKC activity causes flattening and lamellipod extension and limits the magnitude of the initial Ca^{2+} spike. It is likely that other messenger pathways contribute to the response, as indicated by the additional morphological changes that occurred on chemoattractant exposure after pretreatment with 1,2-DOG and by the absence of effects on chemoattractant-induced changes in morphology of cells injected with PKC inhibitors.

In *Dictyostelium*, DAG has effects on the cytoskeleton that are not mimicked by other activators of PKC (Shariff and Luna, 1992). Evidence against this possibility was obtained by exposing four quiescent cells to 50 nM PMA for 2 min before stimulation by chemoattractant (see Fig. 15 *D*). All four cells flattened and extended lamellipods in response to PMA. None of the cells produced a Ca^{2+} response to stimulation, and none polarized and crawled. Morphologically these cells resembled those treated for long periods with EGTA to deplete Ca^{2+} stores, as shown in Fig. 7.

When cells were treated with PKC activators during chemokinesis, $[Ca^{2+}]_i$ declined and locomotion ceased (Gilbert, S. H., K. Perry, and F. S. Fay. 1991. Activators of protein kinase C paralyze locomotion and reduce $[Ca^{++}]_i$ in newt eosinophilic leukocytes. *J. Cell Biol.* 115:279a). However, the Ca^{2+} gradient was still apparent when average $[Ca^{2+}]_i$ had fallen to <50 nM, as shown by the images in Fig. 17. The cell was treated with octanoyl-acetyl-glyceride, and 2 min later $[Ca^{2+}]_i$ was <25 nM in the front of the cell and ~40 nM in the rear.

Discussion

Properties of the Ca^{2+} Response to Stimulation with Spatially Uniform Chemoattractant

On stimulation, spatially averaged $[Ca^{2+}]_i$ in newt eosinophils rose immediately from ≤100 nM to ≥400 nM, and then declined and fluctuated around a mean value of 200 nM. The initial Ca^{2+} spike was insensitive to brief exposure to 5 mM EGTA applied before stimulation but was blocked by longer incubation in EGTA and by sulfated polysaccharides injected

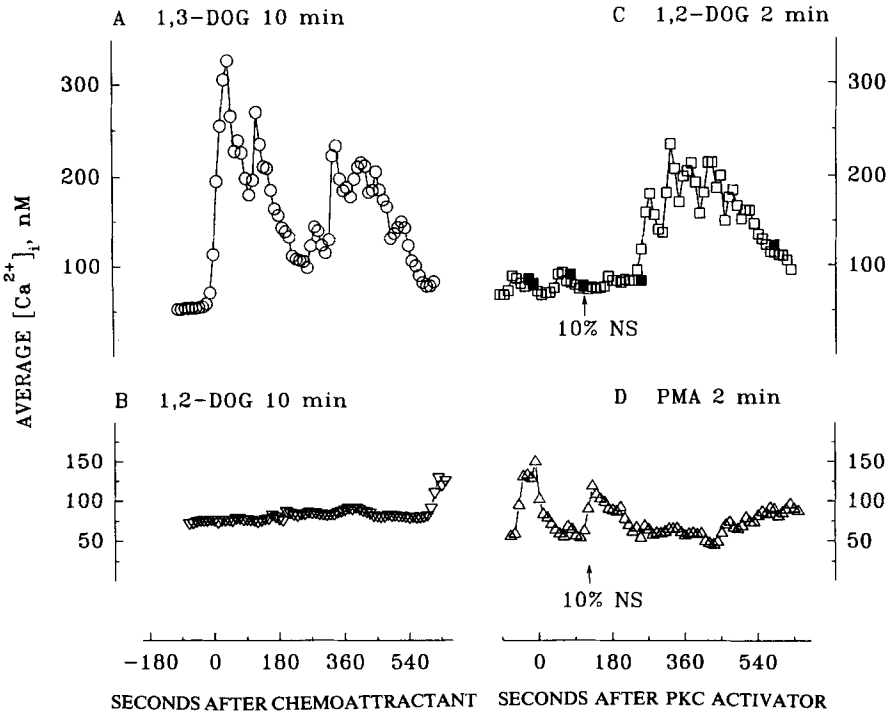

Figure 15. Time courses of $[Ca^{2+}]_i$ responses to activators of PKC and the inactive diacyl glycerol 1,3-DOG. Arrows show times of chemoattractant stimulation (*C* and *D*). Cells were either preincubated in DOG for 10 min before recording (*A* and *B*) or treated during recording for 2 min before stimulation (*C* and *D*). *C* shows $[Ca^{2+}]_i$ for the cell in Fig. 14, with filled symbols corresponding to phase-contrast images. Concentration of diacyl glycerols was 100 μM, of PMA 50 nM.

to intracellular concentrations shown to block $InsP_3$ receptors in other systems (e.g., Ghosh et al., 1988; Hill et al., 1987; Worley et al., 1987; Tones et al., 1989). Active cells treated with 5 mM EGTA continued to produce Ca^{2+} spikes for at least 2 min, but in some cells $[Ca^{2+}]_i$ subsequently declined. The kinetics of the initial Ca^{2+} spike was slowed when fura-2 was injected to final intracellular concentrations above those required to measure $[Ca^{2+}]_i$. SPS injected to low intracellular concentrations, sufficient to block PKC activity in vitro (Herbert and Maffrand, 1991) but below the level required to interfere with $InsP_3$ binding to its receptor (Tones et al., 1989), potentiated the Ca^{2+} response. Injection of a peptide corresponding to the autoinhibitory domain of PKC also potentiated the early Ca^{2+} spike, while preincubation with PKC activators blocked it and suppressed $[Ca^{2+}]_i$ in activated cells.

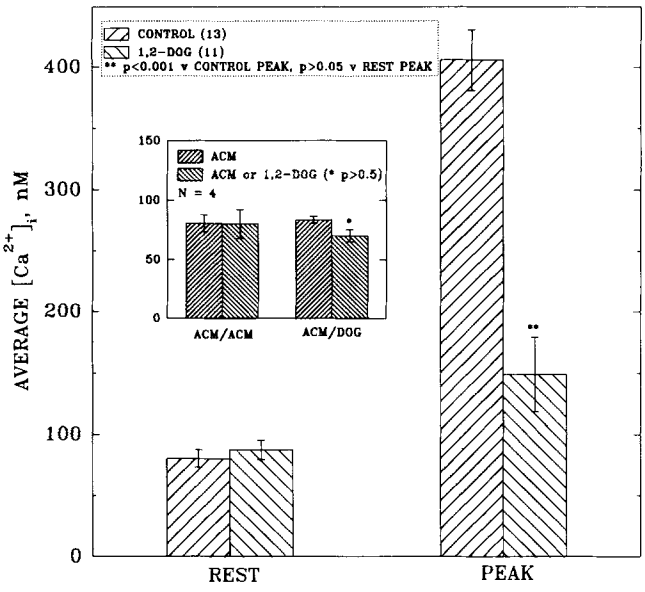

Figure 16. Effects of 1,2-DOG on resting and peak $[Ca^{2+}]_i$. Cells injected with fura-2 were exposed to ACM (*control*) or to ACM containing 100 μM 1,2-DOG for 2 or 10 min. Resting values of $[Ca^{2+}]_i$ were obtained by averaging whole-cell $[Ca^{2+}]_i$ for 1 min before stimulation. The inset shows results obtained in cells whose fluorescence intensity was being recorded when the medium was swapped either for ACM or ACM + 1,2-DOG. The slight difference in $[Ca^{2+}]_i$ before and after DOG treatment of the resting cells is not significant by a Student's *t* test for paired observations.

We conclude from these observations that the first Ca^{2+} spike elicited by stimulation occurs by discharge of internal Ca^{2+} stores and does not require Ca^{2+} influx across the plasma membrane. Inhibition of the response by high concentrations of SPS suggests that at least some of the stores are sensitive to $InsP_3$. The existence of such stores in newt eosinophils is supported by preliminary evidence that $[Ca^{2+}]_i$ is increased by photolysis of caged $InsP_3$ (Gilbert et al., 1994). In this respect newt eosinophils are similar to other electrically inexcitable cells (see Putney, 1993, and references therein).

The simplest interpretation of the results of experiments with activators and inhibitors of PKC is that activity of the enzyme reduces $[Ca^{2+}]_i$ and attenuates the acute Ca^{2+} response to chemoattractant. The postulate that PKC is activated by chemoattractant is suggested by augmentation of the first Ca^{2+} spike in cells injected with agents shown to inhibit PKC in vitro (House and Kemp, 1987; Malinow et al., 1989; Herbert and Maffrand, 1991). In this respect newt eosinophils are like human neutrophils, in which PKC activation inhibits discharge of internal Ca^{2+} stores and activates Ca^{2+} efflux (McCarthy et al., 1989). Alternative interpretations of the observations reported here cannot be ruled out. For example, it is possible that both PKC inhibitors and both PKC activators affect one or more unidentified pathways that

influence Ca^{2+} fluxes in opposite directions independently of PKC activation. The only way to rule out such an interpretation definitively is to develop methods of assaying PKC activity in live single cells.

Spatial Distribution of $[Ca^{2+}]_i$. Ca^{2+} images in Figs. 1 and 9 illustrate that, once the cells were polarized, $[Ca^{2+}]_i$ was always higher in the rear than in the front. The magnitude of the difference was largest at maximal average $[Ca^{2+}]_i$, and a Ca^{2+} gradient was apparent at peak average $[Ca^{2+}]_i$ in these and all other control cells during chemokinesis. It also occurred in cells injected with fura-2 to intracellular concentrations sufficient to damp the kinetics of changes in $[Ca^{2+}]_i$ (i.e., spikes did not occur) and persisted in active cells treated with EGTA, PMA, or diacyl glycerols until $[Ca^{2+}]_i$ was <50 nM (Figs. 7 and 17).

A Ca^{2+} gradient results from a polarized distribution of the relative levels of activity of Ca^{2+} influx and efflux sites. This could result from a polarized distribution of messengers that control Ca^{2+} fluxes or a polarized distribution of the influx and/or efflux sites themselves. The two mechanisms are not mutually exclusive, and, acting together, could reinforce the stability of the Ca^{2+} gradient and possibly the direction of the cell, as discussed below. Observations reported here indicate that polarized messenger distribution is unlikely to be the sole determinant of the Ca^{2+} gradient observed during chemokinesis, when the external stimulus is spatially uniform. For a Ca^{2+} gradient to exist under these conditions, a polarized distribution of Ca^{2+}-controlling messengers would have to result from a polarized distribution of responsive chemoattractant receptors (for which there is evidence in human neutrophils; Sullivan et al., 1984) and/or associated membrane enzymes that produce the messengers. If this were the only gradient-producing mechanism, however, then introducing uniformly into the medium PMA or diacyl glycerols, which suppress $[Ca^{2+}]_i$, might be expected to abolish the Ca^{2+} gradient. This was not observed. Instead these agents caused $[Ca^{2+}]_i$ to fall quickly in active cells during chemokinesis, but the Ca^{2+} gradient persisted until average $[Ca^{2+}]_i$ dropped to ~50 nM, as shown in Fig. 17 (Gilbert, S. H., K. Perry and F. S. Fay. 1991. Activators of protein kinase C paralyze locomotion and reduce $[Ca^{++}]_i$ in newt eosinophilic leukocytes. *J. Cell Biol.* 115:279a). Furthermore, if the Ca^{2+} suppressing action of these agents involved activation of PKC, then the Ca^{2+} gradient should also be abolished by intracellular PKC inhibitors, and this also was not observed, as illustrated in Fig. 9 *C*. If, on the other hand, the Ca^{2+} gradient resulted from a polarized distribution of the targets of chemoattractant-sensitive messengers, whether they were Ca^{2+} stores or efflux/sequestration sites, then treatment with spatially homogeneous agents would not abolish the Ca^{2+} gradient.

Preliminary observations from other recent experiments (Gilbert et al., 1994) support the notion that $InsP_3$-sensitive Ca^{2+} stores are more dense in the rear than in the front of the cell. Cells in which both cytoplasm and internal Ca^{2+} stores were loaded with the acetoxymethyl ester of the low affinity indicator Magfura-2 show a higher ratio of fluorescence intensity at λ_{ex} 340 and 380 in the region near the nucleus and microtubule-organizing center than elsewhere. On the other hand, cells injected with the salt of the same probe show a lower and spatially uniform ratio. Thus there are internal stores of either Mg^{2+} or Ca^{2+} concentrated near the nucleus in newt eosinophils. In other experiments, spatially uniform photolysis of caged $InsP_3$ produced an increase in $[Ca^{2+}]_i$ that was highest in the perinuclear region, suggesting that the divalent cation detected in intracellular compartments of Magfura-2 loaded as the AM ester was more likely to have been Ca^{2+} than Mg^{2+}. This is supported by previous observations of cells loaded with the AM ester of fura-2, revealing a membrane-bounded Ca^{2+} store near the microtubule-organizing center (Brundage et al., 1993).

Effects of $[Ca^{2+}]_i$ and Other Messengers on Cell Morphology, Polarity, and Locomotion

Several methods of perturbing Ca^{2+} homeostasis in these cells were identified by these experiments, and three of them blocked polarization and locomotion but had no effect on flattening and lamellipod formation elicited by chemoattractant (which were blocked by high concentrations of heparin, the fourth Ca^{2+}-perturbing treatment). The three treatments were exposure to EGTA and PKC activators, which abolished or greatly attenuated the Ca^{2+} spike, and injection of fura-2 to high intracellular concentrations, which significantly reduced its rate of rise. The results indicate that the early spike is not required for the initial morphological responses to chemoattractant but is necessary for polarization and locomotion. Furthermore, the abnormal morphological response of the cell injected with excess fura-2 (Figs. 7 *C* and 8 *B*) suggests that the kinetics of the Ca^{2+} response may be important for polarization and locomotion to progress normally. However, processes activated by the early spike are not sufficient for sustained polarity and locomotion in the presence of chemoattractant but low $[Ca^{2+}]_i$, as illustrated by the loss of polarity and motility in cells whose Ca^{2+} responses to chemoattractant were suppressed by treatment with EGTA or PKC activators.

Two PKC inhibitors augmented the acute Ca^{2+} response but had no readily detectable effect on the development of the Ca^{2+} gradient and polarization and locomotion. These observations are consistent with the idea that a polarized distribution of Ca^{2+} stores is sufficient to produce a Ca^{2+} gradient, which in turn promotes polarization and locomotion. Cells whose $[Ca^{2+}]_i$, measured within 1 min of microinjection, was above resting levels flattened, polarized, and crawled normally for several minutes, suggesting that a Ca^{2+} spike alone may be sufficient to initiate these processes in the absence of chemoattractant.

PKC activators, Ca^{2+}, and the cytoskeleton. Cells treated with 1,2-DOG or PMA in the absence of chemoattractant flattened and formed lamellipods, as did cells stimulated with chemoattractant whose acute Ca^{2+} responses had been blocked or altered. These observations suggest that the Ca^{2+}-independent responses of the cytoskeleton to chemoattractant may be mediated by DAG and PKC. Unlike Ca^{2+}, however, this pathway is not sufficient to initiate polarization and locomotion, as indicated by the fact that cells treated with PKC activators did not polarize and crawl.

The experimental evidence suggests that Ca^{2+} homeostasis and morphological responses to chemoattractant are partly controlled by the pathways summarized schematically in Fig. 18. Stimulation appears to release both $InsP_3$ and DAG, and inhibition or potentiation of each of these pathways independently had effects consistent with the conclusion that

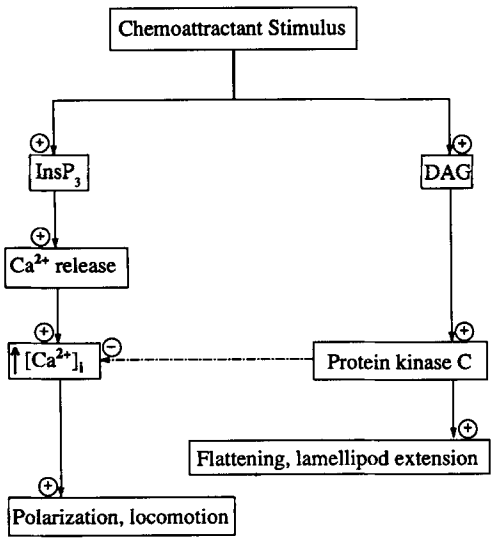

Figure 18. Schematic summary of components of the chemoattractant signal transduction pathway that participates in activation, polarization, and locomotion in newt eosinophils.

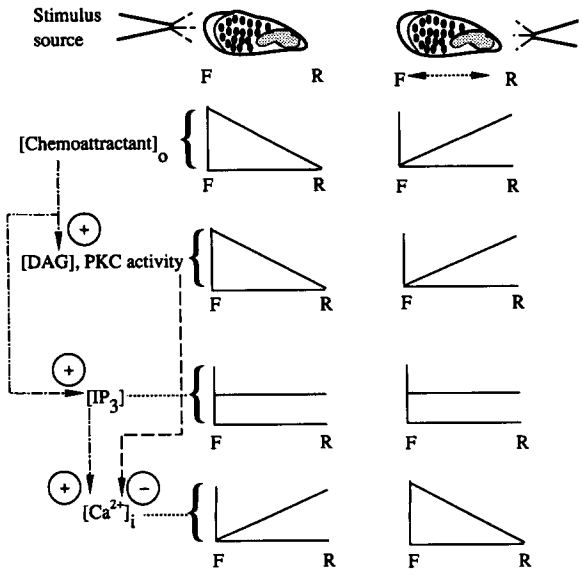

Figure 19. Cartoon illustrating a hypothesis for messenger-mediated reversal of the $[Ca^{2+}]_i$ gradient in response to reversal of the stimulus gradient. The cartoon represents the experiment shown in Fig. 4 *A* of Brundage et al. (1991), in which a puffer pipette used as the source of chemoattractant to lead a newt eosinophil was moved from the front (*F*) to the rear (*R*) of the cell. Beneath the sketches of the cell are graphs showing hypothetical profiles of concentrations of chemoattractant, diacyl glycerol (*DAG*), activated PKC, $InsP_3$, and $[Ca^{2+}_i]$. The proposed signal transduction pathway is shown schematically at the left. In the experiment reported by Brundage et al. (1991), the earliest response to reversing the stimulus gradient was reversal of the $[Ca^{2+}]_i$ gradient. The concentration profiles of DAG, active PKC, and $InsP_3$ are inferred from the effects of these agents on whole-cell $[Ca^{2+}]_i$ and difference in partition coefficients between cytosol and membrane of $InsP_3$ and DAG.

$InsP_3$ through Ca^{2+} activates polarization and locomotion, while DAG through PKC induces flattening and lamellipod formation. The $InsP_3/Ca^{2+}$ pathway appears necessary for polarization and locomotion, and Ca^{2+} alone may be sufficient to elicit these responses transiently. The DAG/PKC pathway alone is sufficient for flattening and lamellipod formation but cannot produce polarization and locomotion in the absence of chemoattractant and may not be necessary for any of these processes to occur on stimulation. The augmentation of the early Ca^{2+} spike by PKC inhibitors suggests that this pathway is activated by the stimulus, but the fact that flattening and lamellipod formation seem to have occurred normally in these cells suggests that as yet unidentified (and perhaps Ca^{2+}-sensitive) pathways can also trigger these responses.

The actin cytoskeleton and its accessory proteins are targets of both PKC and Ca^{2+}, and their interactions are complex. For example, the MARCKS protein (myristolated alanine-rich C kinase substrate; for a recent review see Aderem, 1992) binds to membranes, actin filaments, and the Ca^{2+}-calmodulin complex and exhibits microfilament-bundling activity (Hartwig et al., 1992). Phosphorylation reduces its affinity for membranes, and association with the Ca^{2+}-calmodulin complex, which is inhibited by phosphorylation, disperses microfilament bundles without dissociating MARCKS from individual microfilaments. Therefore MARCKS could respond to both PKC activation and increased $[Ca^{2+}]_i$ by disrupting the organization of microfilaments and their association with membranes and may play a role in converting local changes in $[Ca^{2+}]_i$ and PKC activity to changes in the actin cytoskeleton and locomotion.

The myosins are also targets of Ca^{2+} and PKC. Phosphorylation of nonmuscle myosin II, by PKC as well as the Ca^{2+}-calmodulin/myosin light chain kinase pathway, appears to regulate its function in other systems (Higashihara et al., 1991; Pasternak et al., 1989; Murakami and Elzinga, 1993). Nonmuscle myosin II is regulated by myosin light chain kinase (Cande and Ezzell, 1986), and a bacterial-peptide chemoattractant has been shown to stimulate phosphorylation of the 20-kD myosin light chain in leukocytes (Fechheimer and Zigmond, 1983). Detailed studies of the genetics of type II myosins, especially those of *Dictyostelium* by Spudich and colleagues, show that they play a significant role in both polarization and normal locomotion. Mutants with truncated myosin II (incapable of forming minifilaments) flatten and extend lamellipods in all directions but can neither polarize nor move persistently in one direction (Fukui et al., 1990). Thus Ca^{2+}'s effects on the state of myosin II and the contractile activity of acto-myosin II complexes may contribute to its role in polarization and locomotion.

The $[Ca^{2+}]_i$ Gradient and Cell Polarity

The evidence that the DAG/PKC pathway is activated by the stimulus and has effects on both $[Ca^{2+}]_i$ and the cytoskeleton suggests that both PKC and Ca^{2+} could play key roles in linking directional external signals to intracellular organization during chemotaxis. Furthermore, the possibility that PKC activity affects $[Ca^{2+}]_i$ suggests a mechanism whereby this enzyme might contribute to the reorientation of the $[Ca^{2+}]_i$ gradient when the stimulus source is relocated (Brundage et al., 1991, Fig. 4 *A*), which cannot be explained by a polarized distribution of Ca^{2+} sources and sinks.

As shown by the cartoon in Fig. 19, these events might occur as a consequence of the difference in the spatial distributions of $InsP_3$ and DAG, which have opposite effects on $[Ca^{2+}]_i$. The intracellular mobilities and locations of these messengers are expected to be different because of their different partition coefficients between lipid membranes and aqueous cytoplasm (see Lew, 1989). When the stimulus source is moved from the front (*F*) to the rear (*R*) of the cell, both DAG and $InsP_3$ would be produced by interaction of the chemoattractant with receptors present in the rear (*R*). $InsP_3$ would rapidly equilibrate throughout the cell (Albritton et al., 1992), inducing Ca^{2+} release wherever there are internal stores. DAG would remain in or near membranes close to the stimulus source in the rear. Activated PKC partitions into membranes in many cells (e.g., O'Flaherty et al., 1990; Ito et al., 1988) and could locally suppress $[Ca^{2+}]_i$ (McCarthy et al., 1989), producing a $[Ca^{2+}]_i$ gradient oriented away from the repositioned stimulus (see Poenie et al., 1987).

Superficially, this mechanism might appear to contradict the experimental evidence that the Ca^{2+} gradient during chemokinesis is insensitive to spatially uniform activators and inhibitors of PKC. A fundamental and highly relevant issue, however, is the distinction between chemokinesis, when the stimulus is spatially uniform, and chemotaxis, when the stimulus is graded. We propose that the Ca^{2+} gradient observed during chemokinesis arises primarily from a polarized distribution of Ca^{2+} sources and/or efflux sites and persists in the face of exogenous, spatially uniform agents that suppress or elevate $[Ca^{2+}]_i$. During chemotaxis, however, the Ca^{2+} gradient could reverse when the stimulus gradient is reversed because of a change in the intracellular distribution of stimulus-sensitive messengers that can affect Ca^{2+} fluxes and override the spatial pattern resulting from the physical distribution of Ca^{2+} stores.

Both the $[Ca^{2+}]_i$ gradient and the spatially heterogeneous distribution of activated PKC could have profound effects on the cytoskeleton. Activation of PKC at R near the relocated pipette might destabilize the structure of cortical actin and myosin II, perhaps via MARCKS and myosin II phosphorylation. Also, low $[Ca^{2+}]_i$ in that region could inhibit myosin II activity and favor lamellipod formation and expansion. High $[Ca^{2+}]_i$ near the lamellipod at F could trigger depolymerization of actin microfilaments and destruction of the lamellipodial meshwork, perhaps again through Ca^{2+}-sensitive proteins associated with or having effects on the actin cytoskeleton. Together these regional differences in the composition, structure, and activities of cytoskeletal elements would bring about reorientation of the cell. The existence of a mechanism for redistribution of messengers that control $[Ca^{2+}]_i$ and PKC activity would thus provide the means for initiating reorientation of the cell in response to changes in the direction of the external stimulus. Redistribution of sites of Ca^{2+} influx and efflux initiated by regional changes in the state of the cytoskeleton could then reinforce the spatial gradient of subsequent Ca^{2+} spikes, which would stabilize cytoskeletal organization and sustain the new direction of the cell.

We thank R. Tuft for advice on optics and K. Fogarty, D. Bowman, and R. Naravane for software modifications.

This work was supported by AM37277 and a Career Advancement Award to S. H. Gilbert from the National Science Foundation and by HL14523 to F. S. Fay.

Received for publication 16 August 1993 and in revised form 7 July 1994.

References

Aderem, A. 1992. The MARCKS brothers: a family of protein kinase C substrates. *Cell.* 71:713–716.

Almers, W., and E. Neher. 1985. The Ca signal from fura-2 loaded mast cells depends strongly on the method of dye-loading. *FEBS (Fed. Eur. Biochem. Soc.) Lett.* 192:13–18.

Albritton, N. L., T. Meyer, and L. Stryer. 1992. Range of messenger action of calcium ion and inositol-1,4,5-trisphosphate. *Science (Wash. DC).* 258:1812–1815.

Becker, P. L., and F. S. Fay. 1987. Photobleaching of fura-2 and its effect on determination of calcium concentrations. *Am. J. Physiol.* 253 (*Cell Physiol.* 22) c613–c618.

Brundage, R. A., K. E. Fogarty, R. A. Tuft, and F. S. Fay. 1991. Calcium gradients underlying polarization and chemotaxis of eosinophils. *Science (Wash. DC).* 254:703–706.

Brundage, R. A., K. E. Fogarty, R. A. Tuft, and F. S. Fay. 1993. Chemotaxis of newt eosinophils: calcium regulation of the chemotactic response. *Am. J. Physiol.* 265 (*Cell Physiol.* 34):C1527–C1543.

Cande, W. Z., and R. M. Ezzell. 1986. Evidence for regulation of lamellipodium and tail contraction of glycerinated chicken embryonic fibroblasts by myosin light chain kinase. *Cell Motil. Cytoskeleton.* 6:640–648.

Collins, K., and P. Matsudaira. 1991. Differential regulation of vertebrate myosins I and II. *J. Cell Sci. Suppl.* 14:11–16.

Connor, J. A. 1993. Intracellular calcium mobilization by inositol, 1,4,5-trisphosphate: intracellular movements and compartmentalization. *Cell Calcium.* 14:185–200.

Fechheimer, M., and S. H. Zigmond. 1983. Changes in cytoskeletal proteins of polymorphonuclear leukocytes induced by chemotactic peptides. *Cell. Motil.* 3:349–361.

Fukui, Y., T. J. Lynch, H. Brzeska, and E. D. Korn. 1989. Myosin I is located at the leading edges of locomoting *Dictyostelium* amoeba. *Nature (Lond.).* 341:328–332.

Fukui, Y., A. D. Lozanne, and J. A. Spudich. 1990. Structure and function of the cytoskeleton of a *Dictyostelium* myosin-defective mutant. *J. Cell Biol.* 110:367–378.

Ghosh, T. K., P. S. Eis, J. M. Mulaney, C. L. Ebert, and D. L. Gill. 1988. Competitive, reversible and potent antagonism of inositol 1,4,5-trisphosphate-activated calcium release by heparin. *J. Biol. Chem.* 263:11075–11079.

Gilbert, S. H., J. W. Walker, R. A. Tuft, D. A. Bowman, and F. S. Fay. 1994. Ca^{2+} stores and Ca^{2+} signal polarity in newt eosinophils. *Biophys. J.* 66:A186.

Girard, S., and D. Clapham. 1993. Acceleration of intracellular calcium waves in *Xenopus* oocytes by calcium influx. *Science (Wash. DC).* 260:229–232.

Grynkiewicz, G., M. Poenie, and R. Y. Tsien. 1985. A new generation of Ca^{2+} indicators with greatly improved fluorescence properties. *J. Biol. Chem.* 260:3440–3450.

Hahn, K., R. DeBiasio, and D. L. Taylor. 1992. Patterns of elevated free calcium and calmodulin activation in living cells. *Nature (Lond.).* 359:736–738.

Hartwig, J. H., M. Thelen, A. Rosen, P. A. Janmey, A. C. Nairn, and A. Aderem. 1992. MARCKS is an actin filament crosslinking protein regulated by protein kinase C and calcium-calmodulin. *Nature (Lond.).* 356:618–622.

Herbert, J. M., and J. P. Maffrand. 1991. Effect of pentosan polysulphate, standard heparin and related compounds on protein kinase C activity. *Biochim. Biophys. Acta.* 1091:432–441.

Higashihara, M., K. Takahata, and K. Kurokawa. 1991. Effect of phosphorylation of myosin light chain by myosin light chain kinase and protein kinase C on conformational change and ATPase activities of human platelet myosin. *Blood.* 12:3224–3231.

Hill, T. D., P. Berggren, and A. L. Boynton. 1987. Heparin inhibits inositol trisphosphate-induced calcium release from permeabilized rat liver cells. *Biochem. Biophys. Res. Commun.* 149:897–901.

Hiraoka, Y., J. W. Sedat, and D. A. Agard. 1990. Determination of three-dimensional imaging properties of a light microscope system. *Biophys. J.* 57:325–333.

House, C., and B. E. Kemp. 1987. Protein kinase C contains a pseudosubstrate prototope in its regulatory domain. *Science (Wash. DC).* 238:1726–1728.

Ito, T., T. Tanaka, T. Yoshiba, K. Onoda, H. Ohta, M. Hagiwara, Y. Itoh, M. Ogura, H. Saito, and H. Hidaka. 1988. Immunocytochemical evidence for translocation of protein kinase C in human megakaryoblastic leukemic cells: synergistic effects of Ca^{2+} and activators of protein kinase C on the plasma membrane association. *J. Cell Biol.* 107:929–937.

Janson, L. W., J. Kolega, and D. Lansing Taylor. 1991. Modulation of contraction by gelatin/solation in a reconstituted motile model. *J. Cell Biol.* 114:1005–1015.

Koonce, M. P., R. A. Cloney, and M. W. Berns. 1984. Laser irradiation of centrosomes in newt eosinophils: evidence of centriole role in motility. *J.*

Cell Biol. 98:1999–2010.

Laskin, D., C. Gardner, and J. Laskin. 1987. Induction of chemotaxis in mouse peritoneal macrophages by activators of protein kinase C. *J. Leuk. Biol.* 41:474–480.

Lew, D. P. 1989. Receptor signalling and intracellular calcium in neutrophil activation. *Eur. J. Clin. Invest.* 19:338–346.

Malinow, R., H. Schulman, and R. W. Tsien. 1989. Inhibition of postsynaptic PKC of CaMKII blocks induction but not expression of LTP. *Science (Wash. DC).* 245:862–866.

Marks, P. W., B. Hendey, and F. R. Maxfield. 1991. Attachment of fibronectin or vitronectin makes human neutrophil migration sensitive to alterations in cytosolic free calcium concentration. *J. Cell Biol.* 112:149–158.

McCarthy, S. A., T. J. Hallam, and J. E. Merritt. 1989. Activation of protein kinase C in human neutrophils attenuates agonist-stimulated rises in cytosolic free Ca^{2+} concentration by inhibiting bivalent-cation influx and intracellular Ca^{2+} release in addition to stimulating Ca^{2+} efflux. *Biochem. J.* 245: 357–364.

Moore, E. D. W., P. L. Becker, K. E. Fogarty, D. A. Williams, and F. S. Fay. 1990. Ca^{2+} imaging in single living cells: theoretical and practical issues. *Cell Calcium.* 11:157–179.

Murakami, N., and M. Elzinga. 1993. Phosphorylation of a 47kDa fragment of brain myosin by casein kinase II and protein kinase C. *Biophys. J.* 64:A145.

O'Flaherty, J. T., D. P. Jacobson, J. F. Redman, and A. G. Rossi. 1990. Translocation of protein kinase C in human polymorphonuclear neutrophils. *J. Biol. Chem.* 16:9146–9152.

Pasternak, C., P. F. Flicker, S. Ravid, and J. A. Spudich. 1989. Intermolecular versus intramolecular interactions of *Dictyostelium* myosin: possible regulation by heavy chain phosphorylation. *J. Cell Biol.* 109:203–210.

Poenie, M., R. Y. Tsien, and A.-M. Schmitt-Verhulst. 1987. Sequential activation and lethal hit measured by $[Ca^{2+}]_i$ in individual cytolytic T cells and targets. *EMBO (Eur. Mol. Biol. Organ.) J.* 6:2223–2232.

Pollard, T. D., and E. D. Korn. 1973. *Acanthamoeba* myosin: isolation from *Acanthamoeba castellanii* of an enzyme similar to muscle myosin. *J. Biol. Chem.* 248:4682–4690.

Putney, J. W. 1993. Excitement about calcium signaling in inexcitable cells. *Science (Wash. DC).* ("Perspectives") 262:676–678.

Scanlon, M., D. A. Williams, and F. S. Fay. 1987. A Ca^{2+}-insensitive form of fura-2 associated with polymorphonuclear leukocytes. *J. Biol. Chem.* 262:6308–6312.

Shariff, A., and E. J. Luna. 1992. Diacyglycerol-stimulated formation of actin nucleation sites at plasma membranes. *Science (Wash. DC).* 256:245–247.

Sullivan, S. J., G. Daukas, and S. H. Zigmond. 1984. Asymmetric distribution of the chemotactic receptor on polymorphonuclear leukocytes. *J. Cell Biol.* 99:1461–1467.

Taylor, D. L., J. R. Blinks, and G. Reynolds. 1980. Contractile basis of ameboid movement. I. Aequorin luminescence during ameboid movement, endocytosis and capping. *J. Cell Biol.* 86:599–607.

Tones, M. A., M. D. Bootman, B. F. Higgins, D. A. Lane, G. F. Pay, and U. Lindahl. 1989. The effect of heparin on the inositol 1,4,5-trisphosphate receptor in rat liver microsomes. *FEBS (Fed. Eur. Biochem. Soc.) Lett.* 242:105–108.

Worley, P. F., J. M. Baraban, S. Supattapone, V. S. Wilson, and S. H. Snyder. 1987. Characterization of inositol trisphosphate receptor binding in brain: regulation of pH and calcium. *J. Biol. Chem.* 262:12132–12136.

Thorn, P., A. M. Laurie, P. M. Smith, D. V. Gallagher, and O. H. Petersen. 1993. Ca^{2+} oscillations in pancreatic acinar cells: spatiotemporal relationships and functional implications. *Cell Calcium.* 14:746–757.

Yin, H. L., and T. P. Stossel. 1979. Control of cytoplasmic actin gel-sol transformation by gelsolin, a calcium-dependent regulatory protein. *Nature (Lond.).* 281:583–586.

Zimmermann, P. G., and H. U. Keller. 1988. Diacylglycerol-induced shape changes, movements and altered F-actin distribution in human neutrophils. *J. Cell Sci. Suppl.* 90:657–666.